Scenario changes in the climatology of winter midlatitude cyclone activity over eastern North America and the Northwest Atlantic

Z. Long,[1] W. Perrie,[1,2] J. Gyakum,[3] R. Laprise,[4] and D. Caya[5,6]

Received 28 July 2008; revised 15 March 2009; accepted 17 April 2009; published 23 June 2009.

[1] The present study explores how midlatitude winter cyclone activity can be modified under warming-induced conditions due to enhanced greenhouse gas concentrations. We performed simulations with the Canadian Regional Climate Model (CRCM version 3.5) implemented on a domain that covers the Northwest Atlantic and eastern North America. These simulations are driven by control conditions (1975–1994) and high-CO_2 scenario conditions (2040–2059) suggested by the Canadian Climate Centre model, CGCM2 (Second Generation Coupled Global Climate Model), following the IPCC IS92a scenario. Comparisons between model simulations for the control period (1975–1994) and North America Regional analysis (NARR) suggest that both CGCM2 and CRCM reliably reproduce the overall NARR patterns of sea level pressure, tropospheric baroclinicity and Atlantic storm tracks. However, compared to CGCM2 results, CRCM offers an improvement in simulations of the most intense cyclones. Although both models underestimate the track density of intense cyclones, the CGCM2 underestimates are larger than those of CRCM. Under the high-CO_2 climate change scenario, the CRCM and CGCM2 model simulations show similar changes in sea level pressure, surface temperature, and total track density of midlatitude winter cyclones. Although we can see the northwest shift of the dominant Atlantic storm track, it is not statistically significant. Moreover, simulations from both models show a decrease in the total cyclone track density along the Canadian east coast; the decrease is more robust in CRCM simulations than in CGCM2 results. For intense cyclones, CRCM simulations show a slight decrease in the track density, while no such change is found in CGCM2 simulations.

Citation: Long, Z., W. Perrie, J. Gyakum, R. Laprise, and D. Caya (2009), Scenario changes in the climatology of winter midlatitude cyclone activity over eastern North America and the Northwest Atlantic, *J. Geophys. Res.*, *114*, D12111, doi:10.1029/2008JD010869.

1. Introduction

[2] Midlatitude cyclones are responsible for much of the poleward transport of atmospheric heat and moisture. Intense midlatitude cyclones have potential impact on North American coastal areas because they are often associated with high winds, heavy precipitation and high ocean surface waves. Therefore any potential change in the climate of these cyclones is of great interest to society, given the large population densities in these areas and the possible economic impacts. In the present study, we are concerned with the impacts of climate change on midlatitude winter cyclones.

[3] In high-CO_2 climate change scenarios, studies suggest that changes in midlatitude cyclone frequency may be related to reductions in the north-south temperature gradients in the lower troposphere [*Zhang and Wang*, 1997; *Carnell and Senior*, 1998; *Lunkeit et al.*, 1998; *Knippertz et al.*, 2000]. The largest lower tropospheric warming is expected to occur over northern polar regions in winter. However, warming does not occur uniformly throughout the atmosphere. In the upper troposphere, temperatures in the tropical regions are expected to increase faster than those in polar areas [*Meehl et al.*, 2007]. Therefore a competitive situation is developed. While enhanced greenhouse warming reduces lower tropospheric baroclinicity, it also increases the upper tropospheric meridional temperature gradient and provides more energy to activate midlatitude cyclones. Moreover, there are additional factors; in addition to the changes in baroclinicity, globally averaged mean water vapor is projected to increase [*Meehl et al.*, 2007], which is expected to provide a secondary energy source for midlatitude storms [*Carnell and Senior*, 1998; *Lambert*, 2004]. However, because

[1]Fisheries and Oceans Canada, Bedford Institute of Oceanography, Dartmouth, Nova Scotia, Canada.
[2]Department of Engineering Math, Dalhousie University, Halifax, Nova Scotia, Canada.
[3]Department of Atmospheric and Oceanic Sciences, McGill University, Montreal, Quebec, Canada.
[4]Département des Sciences de la Terre et de l'Atmosphère, Université du Québec à Montréal, Montréal, Québec, Canada.
[5]Centre pour l'Étude et la Simulation du Climat à l'Échelle Régionale (ESCER), Université du Québec à Montréal, Montréal, Québec, Canada.
[6]Ouranos Consortium, Montréal, Québec, Canada.

studies have shown that baroclinic wave activity is more sensitive to lower level changes rather than changes in the upper troposphere [*Held and O'Brien*, 1992; *Lunkeit et al.*, 1998], it is therefore reasonable to expect a reduction in the frequency of midlatitude cyclones under enhanced greenhouse warming conditions.

[4] Further studies of the response of midlatitude cyclones to climate change scenarios with GCMs (General Circulation Models) have shown trends that are consistent with the results cited here. In terms of cyclone count [*Lambert*, 1995; *Lambert*, 2004; *Zhang and Wang*, 1997; *Carnell and Senior*, 1998] or track density [*Sinclair and Watterson*, 1999; *Bengtsson et al.*, 2006], there is a statistically significant reduction in the total number of winter cyclones in a warmer climate. In addition, some GCM simulations suggest that a warmer climate may cause the North Atlantic storm tracks to shift poleward [*Schubert et al.*, 1998; *Lunkeit et al.*, 1998; *Ulbrich and Christoph*, 1999; *Knippertz et al.*, 2000]. Therefore winter midlatitude cyclone activity is estimated to increase in the downstream regions of the principal North Atlantic storm tracks, near Europe, and decrease in the source regions near North America.

[5] However, there is still uncertainty concerning the possible impacts of climate warming scenarios on the intensity (in terms of minimum sea level pressure) of midlatitude cyclones [*Meehl et al.*, 2007]. For example, *Lambert* [1995, 2004] reported that the number of intense extratropical cyclones tends to increase under enhanced greenhouse warming [*Lambert*, 2004], but *Sinclair and Watterson* [1999] found a marked decrease in the occurrence of intense storms as deduced from atmospheric vorticity. These discrepancies can be related to many factors, but the probable factors are related to the fact that the storm tracks shift to the regions with preferential lower pressure in a warmer climate and that vorticity is less influenced by changes in the large-scale background. In addition, models differ in physical parameterizations, resolution, dynamics, and also in their representations of the ocean. The coarse resolutions used in GCMs are not sufficiently fine to allow the existence of strong surface pressure gradients to reliably represent extratropical cyclones [*Blender and Schubert*, 2000]. Until recently, high-resolution GCM simulations needed to improve the representation of cyclones, tended to involve experiments that were often too short to provide robust signals of change in the cyclone climate [*Beersma et al.*, 1997]. However, there are several recent studies using high-resolution GCMs to simulate extratropical cyclones [*Geng and Sugi*, 2003; *Bengtsson et al.*, 2007; *Bengtsson et al.*, 2009]. For example, *Bengtsson et al.* [2007] and *Bengtsson et al.* [2009] have recently completed high-resolution model studies, integrated for 30 year periods in time slice mode, to look at tropical and extratropical cyclones. In addition, new high-resolution coupled models are also being developed, for example HIGEM [*Shaffrey et al.*, 2009].

[6] Recent studies suggest that regional climate models (RCMs) are a potential alternative to GCMs for climate change studies at smaller scales [*Pan et al.*, 2001; *Laprise et al.*, 2003; *Plummer et al.*, 2006]. RCMs can be run for long periods of time at relatively high resolutions at an affordable computational cost, implemented on a limited area domain and driven with atmospheric data simulated by a GCM. Studies with the Canadian Regional Climate model (CRCM) show that it has skill in downscaling large-scale information to regional scales and in successfully reproducing the means and variations of a number of fields, such as SLP and precipitation [*Denis et al.*, 2002]. In addition, RCMs have been successfully implemented to investigate possible changes in the future cyclone climatology [*Muskulus and Jacob*, 2005; *Lionello and Giorgi*, 2007; *Semmler et al.*, 2008]. Simulations with the Rossby Center regional climate model RCA2 suggest an 18% decrease in the extratropical cyclone count for the North Atlantic under the SRES-A2 scenario [*Semmler et al.*, 2008]. However, RCMs also have disadvantages. For example, they are typically one-way nested where there is no possibility for feedback to the driving GCM.

[7] Here we are concerned with the possible impacts of climate change on midlatitude cyclones over the North Atlantic and eastern North America. In this paper, we (1) implement CRCM to simulate the cyclone climate over the Northwest Atlantic, (2) validate results from both CRCM and CGCM2 (Second Generation Coupled Global Climate Model) against reanalysis data for the control climate period, and (3) discuss the climate change signal in the two models and the impacts of higher resolution simulations. Section 2 briefly describes CRCM and the experimental design. Section 3 outlines the objective methodology used in tracking extratropical cyclones. Section 4 validates the CRCM simulations of the control storm climate. Section 5 compares the control storm climate with that of the future climate change scenario and section 6 presents the conclusions.

2. Models and Experimental Setup

[8] The regional climate model used for this study is CRCM version 3.5 [*Caya and Laprise*, 1999; *Laprise et al.*, 2003; *Caya and Biner*, 2004]. It is based on the dynamical formulation of the Canadian Mesoscale Compressible Community (MC2) model, and solves the fully elastic nonhydrostatic Euler equations using a semi-implicit semi-Lagrangian numerical scheme. CRCM employs polar-stereographic coordinates in the horizontal and Gal-Chen terrain-following levels in the vertical [*Gal-Chen and Sommerville*, 1975]. Most of the physical parameterization package of the second-generation Canadian Global Climate Model (CGCM2) is implemented within CRCM to represent the subgrid-scale processes [*McFarlane et al.*, 1992]. The Kain-Fritsch scheme was chosen for deep convection while large-scale condensation is simulated using the CGCM2 physics formulation [*Kain and Fritsch*, 1990; *Paquin and Caya*, 2000]. A detailed description of CRCM version 3.5 is given by *Caya and Laprise* [1999], *Laprise et al.* [2003] and *Caya and Biner* [2004].

[9] In this study, the CRCM model domain is centered over the western North Atlantic and covers most of eastern North America (Figure 1). Since this domain excludes the northwest Pacific and the Rockies where eastward cyclones tend to originate, the CRCM results depend solely on the information from CGCM2 for those cyclones, and cyclogenesis in the lee of the Rockies is potentially not well resolved. However, comparisons with NARR simulations

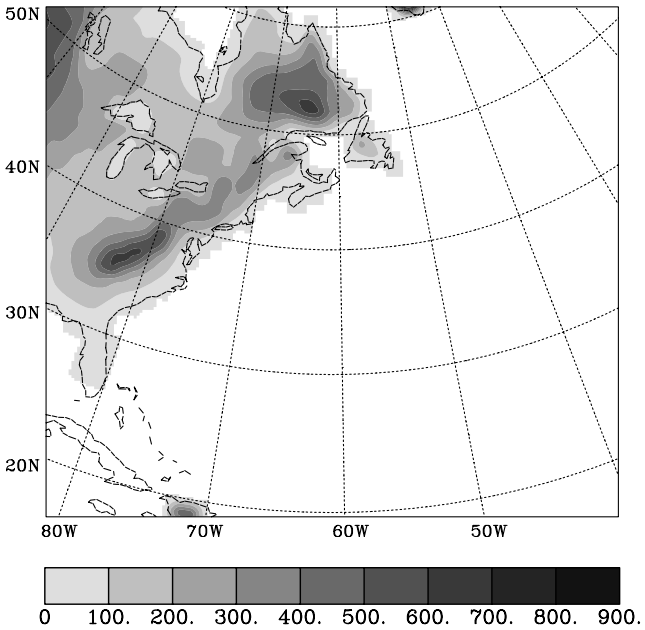

Figure 1. CRCM domain and topography. Interval: 100 m.

suggest that CGCM2 results capture the eastward storm tracks well, except for a slight overestimation in storm frequency (Figure 4). The CRCM simulations were performed at a horizontal resolution of 30 km with 203 × 181 grid points. In the vertical direction, there are 18 levels. A 15-min time step is employed. The simulations were conducted for two 20-year slices, representing the present or control climate (1975–1994) and high-CO_2 scenario conditions (2040–2059). Sea surface temperatures and sea ice coverage are interpolated from CGCM2 ocean data. The initial fields and lateral boundary conditions used to nest CRCM are taken from a CGCM2 simulation, archived at 6-hourly intervals [*Flato et al.*, 2000; *Flato and Boer*, 2001]. The CGCM2 simulation is for the period from 1850 to 2100 forced with GHG (greenhouse gas) concentrations and aerosol loadings suggested by *Mitchell et al.* [1995], following the IPCC IS92a scenario. The IS92a scenario uses effective greenhouse gas forcing fields corresponding to those observed from 1850 to 1990, with an assumed climate change corresponding to a CO_2 increase of 1% per year thereafter until year 2100. Climate change simulations based on this scenario have been performed by a number of climate modeling groups who have contributed to the IPCC Third Assessment Report.

[10] The atmospheric component of CGCM2 is a spectral model with T32 truncation and 10 unequally spaced vertical hybrid sigma pressure levels. Although 10 vertical levels are fewer than comparable models, CGCM2 has been shown to successfully reproduce the broad features of mean climate variables [*Flato et al.*, 2000; *Lambert*, 1995, 2004]. The ocean component of CGCM2 is GFDL MOM version 1 [*Pacanowski et al.*, 1993] using a 1.875° longitude-latitude horizontal resolution and 29 vertical levels. The sea-ice component of CGCM2 is based on the cavitating fluid sea-ice dynamics scheme of *Flato and Hibler* [1992]. More details about CGCM2 are given by *Flato et al.* [2000] and *Flato and Boer* [2001].

[11] To validate the CRCM simulations, we present comparisons that include data from the North American Regional Reanalysis (NARR) and CGCM2 simulations. NARR is a dynamically consistent, high-resolution, high-frequency, atmospheric and land surface hydrology data set for the North American domain and adjoining regional seas (*Mesinger et al.* [2006]; http://www.emc.ncep.noaa.gov/mmb/rreanl/). NARR has a horizontal resolution of 32 km, 45 vertical levels, and is available for the period 1979 to the present. NARR has higher resolution and accuracy than the corresponding global NCEP/NCAR reanalysis. Some of the most important improvements of NARR are that it is based on an Eta regional model and it is based on a 3-hourly three-dimensional Var data assimilation system, combined with advanced assimilation of precipitation, radiances, additional source data, and improvements to the detailed NOAA land-surface model. Although the data are available for all seasons, we focus on the winter midlatitude cyclones (December–February). To estimate significance levels, we use the Student t test following *Lambert* [1995]. The t statistic is computed using

$$t = \frac{\overline{x_2} - \overline{x_1}}{\left\{\left(\frac{1}{n_2} + \frac{1}{n_1}\right)\left[(n_2 - 1)s_2^2 + (n_1 - 1)s_1^2\right]\right\}^{1/2}}$$

where $\overline{x}$ is a twenty-season mean, s is the standard deviation and n is the number of values. $\overline{x}$ and s are calculated using the 6-hourly data. Subscripts 1 and 2 refer to the two sets of data.

3. Storm Detection and Tracking Methodology

[12] In this study, 6-hourly SLP fields are used to detect and track midlatitude cyclones. The traditional approach is that midlatitude cyclones are identified as pressure minima [*Gulev et al.*, 2001; *Zolina and Gulev*, 2002; *Bauer and Genio*, 2006; *Wernli and Schwierz*, 2006]. However, in regions with a high background pressure gradient, cyclones tend to take the form of a pressure trough rather than a closed minimum. Moreover, because of the strong large-scale background steering flow, these cyclones move quickly and the traditional SLP-based tracking algorithms are therefore biased toward slow-moving systems [*Sinclair*, 1994; *Sinclair and Watterson*, 1999]. To avoid this background flow bias, some studies suggest using vorticity or filtered SLP fields to track midlatitude cyclones [*Sinclair and Watterson*, 1999; *Hoskins and Hodges*, 2002; *Anderson et al.*, 2003; *Hodges et al.*, 2003]. Alternately, high-resolution data can significantly reduce the bias related to the flow dependence on cyclone identification [*Zolina and Gulev*, 2002]. However, the dependence of the intensities on the background is still unresolved. For the intensities determined from raw pressure, pressure gradient or geostrophic vorticity are better measures, and this should be kept in mind when cyclone intensities are discussed in sections 4 and 5.

[13] Prior to cyclone detection and estimation of storm track densities, the SLP fields from NARR and the CGCM2 simulations are interpolated onto the 30-km CRCM grids, using cubic interpolation. For NARR data, the errors generated by this interpolation are small because the latter

have similar horizontal resolution to CRCM. However, when coarse resolution CGCM2 data are interpolated onto high-resolution grids, some storm tracks occur in interpolated high-resolution data that do not exist in the coarse resolution CGCM2 outputs [see also *Blender and Schubert*, 2000]. In areas near the track density maximum, overestimates from the interpolation are as much as 15%. Clearly, the CGCM2 cyclone tracks have to be regarded with caution because of the coarse horizontal resolution (about 500 km).

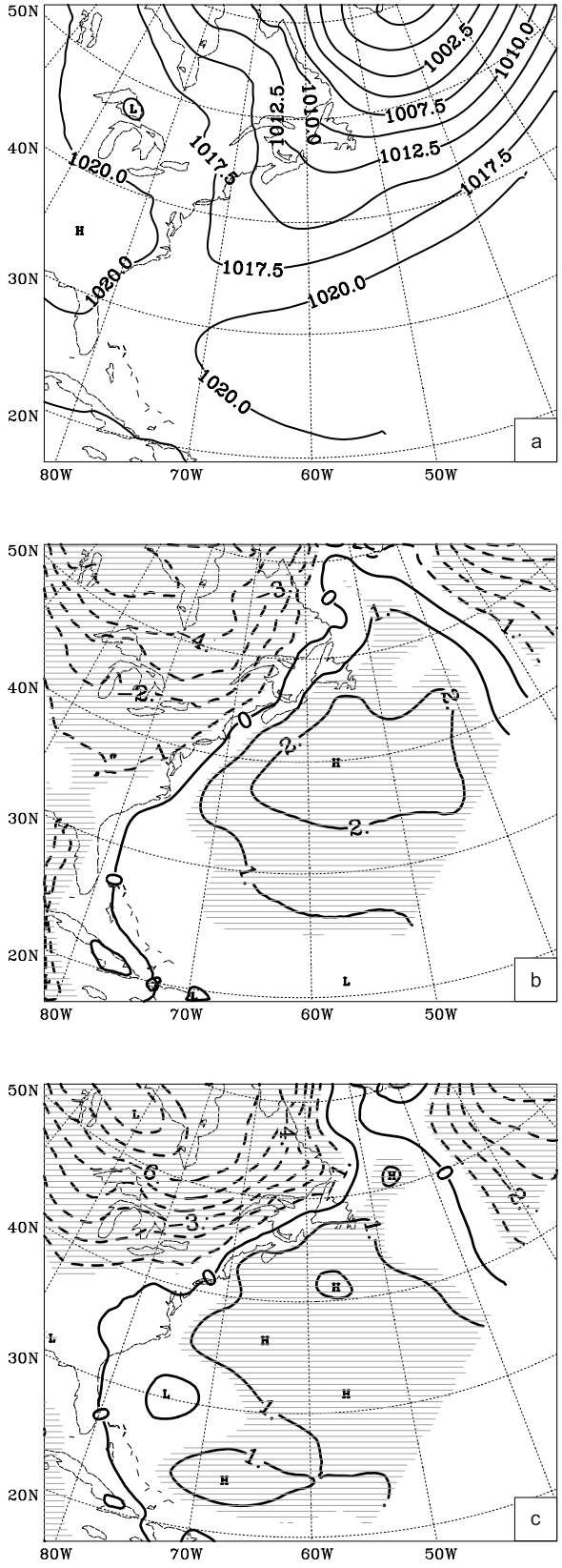

[14] In our approach to storm detection and tracking, we first screen the SLP fields to identify local minima on our polar stereographic grid. A candidate SLP center must satisfy the following criteria.

[15] 1. Local minimum of less than 1010 hPa within a radius of 240 km;

[16] 2. At least one closed isobar on a 4 hPa increment. Tests with differing isobar increments such as 3 hPa and 5 hPa yield similar results. Secondly, we use a simple nearest neighbor search in order to track the individual cyclones from the preceding (6 h) time step. If a cyclone falls within 600 km of a cyclone from a preceding time step, it is assumed to be a continuation of the previous cyclone. Otherwise it is considered a new cyclone. A candidate SLP center is required to have a lifetime of at least 24 h.

[17] We use "track density" to measure the midlatitude cyclone activity following *Sinclair and Watterson* [1999]. Track density is defined as the number of midlatitude cyclone tracks passing any given grid point. In some studies [*Lambert*, 1995; *Lambert*, 2004; *Knippertz et al.*, 2000], the cyclone frequency is calculated as the sum of cyclone events at each grid point, where an event is defined as an occurrence of a low-pressure system at each grid point. As a result, a slowly moving system may be counted many times at a given grid point, while a fast moving system may not be counted at all. Here the cyclone numbers are determined by counting the cyclone occurrences that are connected to their trajectories. Each cyclone is counted just once, per track, per grid point. Thus multicounting at a given grid point is avoided. Following earlier studies [*Carnell and Senior*, 1998; *Hoskins and Hodges*, 2002; *Hodges et al.*, 2003], we scale the track density to the number per season per unit area, where the unit area is about 920,000 km^2.

4. Present (Control) Climate

4.1. SLP Comparisons

[18] The 20-year averaged SLP fields for December–February from the CRCM and CGCM2 model simulations are compared with NARR data in Figures 2a–2c. The overall positions and magnitudes of the subtropical high and the Icelandic Low shown in NARR data are well reproduced by both models. Both models have a tendency to overestimate SLP over the Northwest Atlantic and underestimate SLP near the Hudson Bay region, which may be related to the fact that CGCM2 overestimates

Figure 2. (a) Winter (DJF) SLP for NARR and (b) difference between CRCM simulations minus NARR. Isoline spacing is 2.5 hPa for Figure 2a and 1 hPa for Figure 2b. Light hatching indicates 95% significance level with Student's t-test. (c) Winter (DJF) SLP for difference between CGCM2 simulations minus NARR. Isoline spacing is 1 hPa. Light hatching indicates 95% significance level with Student's t test.

surface air temperatures at high latitudes [*Flato et al.*, 2000]. Over the Hudson Bay region, CRCM achieves a slightly improved SLP simulation relative to NARR data and CGCM2 results, with a maximum SLP bias that is about 3 hPa less than that of CGCM2. The weak low-pressure system over the Great Lakes seen in NARR data is absent in both simulations, which follows from the fact that the Great Lakes are not explicitly present in either model simulation. Over the Northwest Atlantic, the SLP bias from CRCM is 1 hPa higher than that of CGCM2.

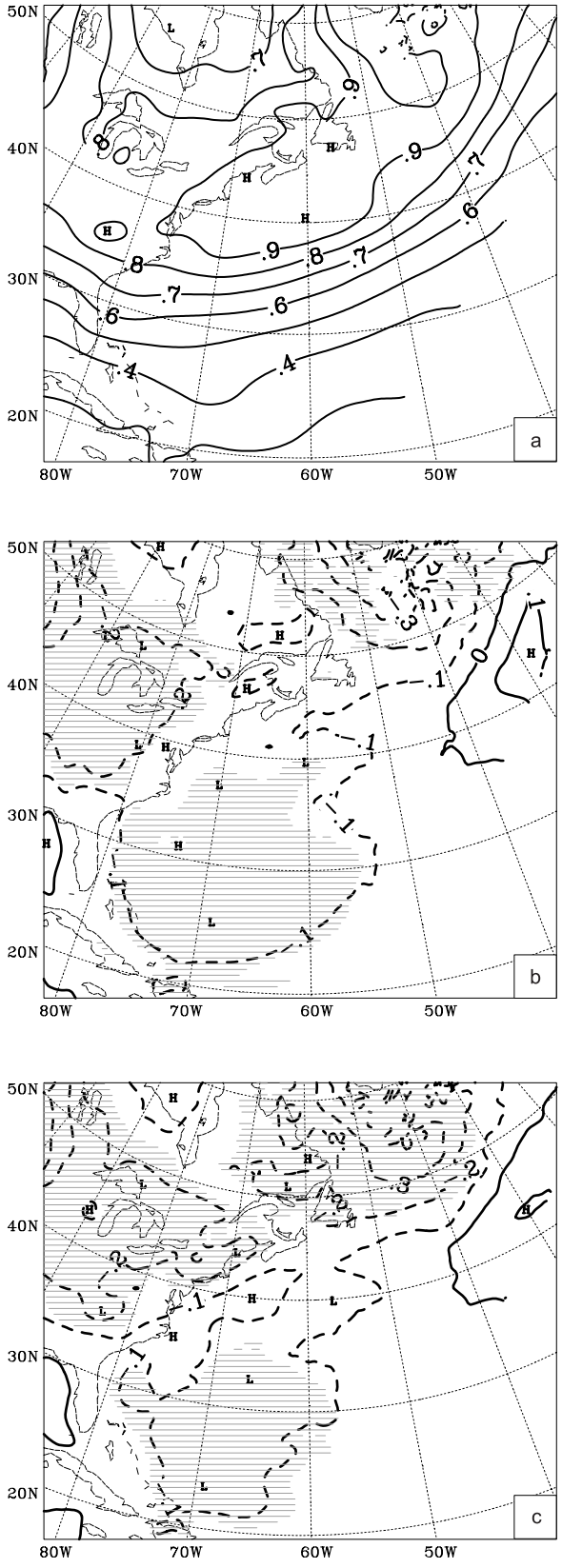

4.2. Baroclinicity

[19] Baroclinic instability provides energy for the development and maintenance of midlatitude cyclones. To quantify baroclinic instability strength, the maximum Eady growth rate is calculated following the traditional methodology [*Lindzen and Farrell*, 1980; *Hoskins and Valdes*, 1990]. The Eddy growth rate is defined as $\sigma = 0.31(f/N)|\partial V/\partial Z|$ where f is the Coriolis parameter, N is the static stability, Z is the vertical height and V is the horizontal wind vector. We estimate σ from 6-hourly fields of wind, temperature and geopotential height at 700 hPa and 850 hPa (Figures 3a–3c). Comparisons between the two models and the NARR data suggest that the coarse resolution CGCM2 is capable of simulating the main features of lower tropospheric baroclinicity. Although both models reliably produce the distinct maximum along the North American east coast seen in the NARR data, both slightly underestimate the baroclinicity maximum by about 0.1–0.2 day^{-1}. In the upper troposphere, we used the 6-hourly data at 250 hPa and 500 hPa to calculate σ and we found no essential difference in the two models (not shown). Both successfully simulate a maximum in baroclinicity between 30°N and 50°N, which is biased slightly to the northeast of the observed maximum in NARR data.

4.3. Track Density of Midlatitude Cyclones

[20] The storm track density from NARR data is shown in Figure 4a. Comparisons between Figure 4a and previous studies [*Zisha and Smith*, 1980; *Gulev et al.*, 2001; *Zolina and Gulev*, 2002; *Hoskins and Hodges*, 2002; *Hodges et al.*, 2003] suggest that our methodology for detecting and tracking cyclones can successfully estimate the storm track maximum along the east coast, with some slight differences in the magnitudes. The overall NARR patterns in Figure 4a are similar to those obtained by *Gulev et al.* [2001] and *Zolina and Gulev* [2002], using unfiltered SLP fields (without removal of large-scale background SLP systems). Because our storm track maximum over the Great Lakes is weak compared to other studies, in part because of the restricted CRCM domain whereby cyclogenesis in the lee of the Rockies is not well resolved, our results should be viewed with caution in that region [*Hoskins and Hodges*, 2002; *Hodges et al.*, 2003; *Zisha and Smith*, 1980].

Figure 3. (a) Winter (DJF) averaged maximum Eady growth rate estimated from the data at 700 and 850 hPa for NARR and (b) difference between CRCM simulations minus NARR. The light shading indicates 95% significance level with Student's t-test. Isoline spacing is 0.1 day^{-1}. (c) Winter (DJF) averaged maximum Eady growth rate estimated from the data at 700 and 850 hPa for the difference between CGCM2 simulations minus NARR. The light shading indicates 95% significance level with Student's t-test. Isoline spacing is 0.1 day^{-1}.

[21] Track density simulations from CRCM and CGCM2 are shown in Figures 4b–4c. They also locate the storm track maximum off the east coast, consistent with the dominant results suggested by the NARR data (Figure 4a). Although both models slightly overestimate a weak maximum over the Great Lakes and simulate the west-east storm track from the Great Lakes to the Canadian east coast, these results are biased slightly to the north of the NARR data. Comparisons of CRCM and CGCM2 track densities to NARR data are displayed as differences in Figures 4b–4c. While track densities are slightly underestimated by CRCM along the east coast of North America, they are significantly underestimated by CGCM2. Moreover, because CGCM2 results are interpolated to relatively high resolution and give about 15% more cyclones than occur in the original CGCM2 data, the underestimation in original CGCM2 data is even larger. Over the Labrador Sea, the track densities are overestimated by CRCM and underestimated by CGCM2. CRCM overestimates are significant for longitudes east of Greenland and north of 45°. Over the Hudson Bay region, overestimates occur in results from both models.

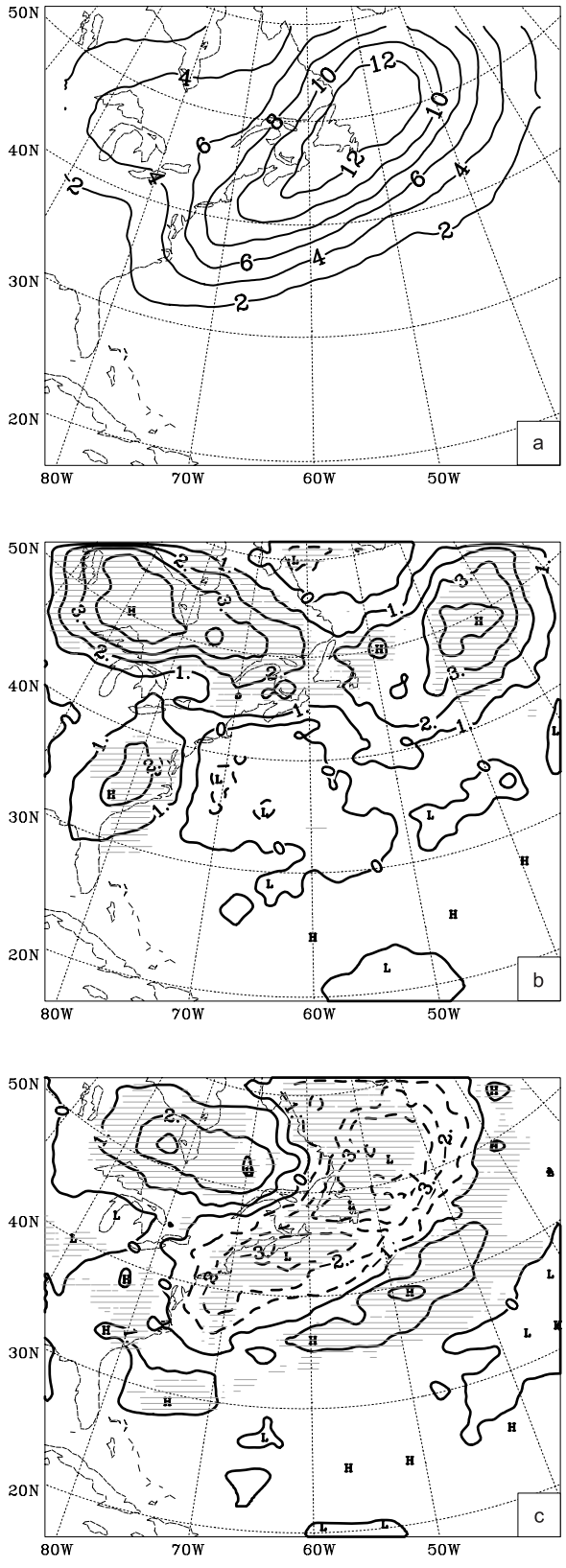

Figure 4. (a) Track densities of total extratropical cyclones from NARR and (b) difference of track densities between model simulations minus NARR for CRCM. Light hatching indicates 95% significance level with Student's t-test. Interval is 2 events per winter for Figure 4a and 1 events per winter for Figure 4b. (c) Difference of track densities between model simulations minus NARR for CGCM2. Light hatching indicates 95% significance level with Student's t-test. Interval is 1 event per winter.

[22] To further understand the relation between the baroclinicity and track densities, Figure 5 shows the 6-year composite Eady growth rate during the years when the highest cyclone track densities occur, for NARR data and the two simulations. Figure 5 shows that during these years, the baroclinicity is significantly stronger at middle latitudes, compared to other regions. Although CRCM and CGCM2 show similar positive baroclinicity anomalies in midlatitudes in overall agreement with NARR data, these simulated positive maxima are located slightly to the south of that seen in the NARR data.

4.4. Intensity of Midlatitude Cyclones

[23] In terms of peak cyclone intensity, NARR data and both models suggest that the majority of midlatitude cyclones are shallow cyclones, with most cyclones achieving between 985 hPa and 995 hPa (Figure 6). Compared to NARR, CRCM underestimates the number of intense cyclones and overestimates the number of weak cyclones, with minimum SLP > 975. By comparison, CGCM2 more seriously underestimates the numbers of intense cyclones than CRCM, although its estimates of weak cyclones are more comparable to NARR data.

[24] Results from NARR, as well as from both models show that most intense midlatitude cyclones (with central pressure lower than 970 hPa) follow the usual Northwest Atlantic storm track. The 970 hPa criterion is chosen as a threshold, following the study by *Lambert* [2004]. Compared to NARR data, both models underestimate the track density of intense cyclones. The bias is about 2 events per season in CRCM results, whereas it is 4 events per season in CGCM2 results (Figure omitted). Overall, the NARR and CRCM track density distributions are similar. Because CRCM and CGCM2 have many of the same physical

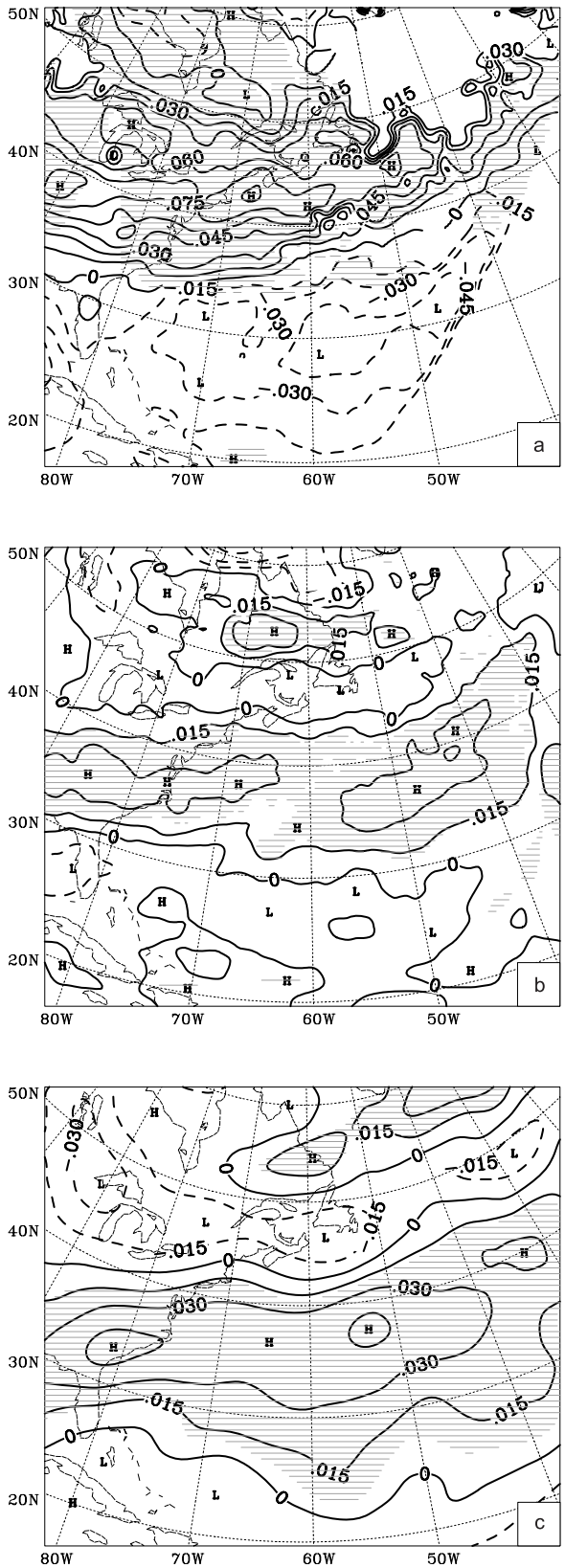

Figure 5. ADY growth rate composite for the 6 years when there are most total cyclone counts for (a) NARR and (b) CRCM. The light shading indicates 95% significance level with Student's t-test. Isoline spacing is 0.015 day^{-1}. (c) EADY growth rate composite for the 6 years when there are most total cyclone counts for CGCM2.

parameterizations, the suggestion that CRCM has smaller bias than CGCM2 could be related to higher resolution in the simulations. Moreover, because the track density for intense cyclones is smaller in CRCM results than in NARR data and because both have similar resolutions, we suggest that CRCM may not represent the physics of intense cyclones as fully as they are represented in NARR data. In addition, as shown in Figure 3, the weak baroclinicity simulated by CRCM may also contribute to this underestimation.

5. Impacts of Climate Change

5.1. SLP and Sea Surface Temperature

[25] It is important to understand the impacts of climate change on the surface of the Northwest Atlantic, because midlatitude cyclonic activity is dominated by lower troposphere baroclinicity [*Held and O'Brien*, 1992; *Lunkeit et al.*, 1998]. Under the IPCC IS92a scenario, both models exhibit similar changes in SLP and surface temperature, comparing the control and high-CO_2 climate simulations (Figures 7–8). This is to be expected, since the regional CRCM model is forced by the same SST, and over water, the surface temperature is strongly tied to the SST. The greatest lowering in SLP occurs where the largest warming is simulated to take place, which is over high-latitude land, flanked on the east by an area of weak cooling over the Labrador Sea. Studies suggest that this cooling is probably due to reduced poleward heat transport associated with a weakened thermohaline circulation [*Stouffer*, 2004]. GCM simulations show a similar signal in the central Atlantic [*Meehl et al.*, 2007]. Since the ocean is warmer than nearby land in winter, this warming pattern implies a decrease in temperature gradient along the east coast of North America,

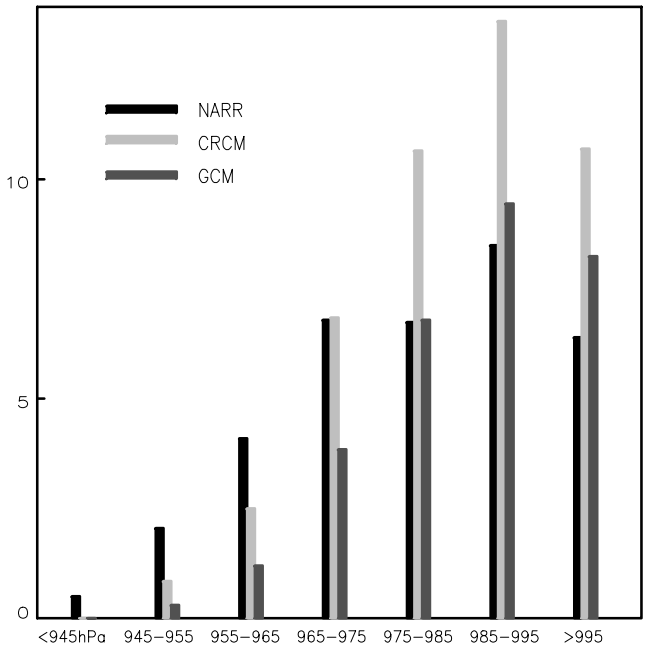

Figure 6. Current climate in terms of minimum SLP for extratropical cyclones simulated by CGCM2, CRCM, and NARR, expressed in storm events per winter over the whole CRCM domain.

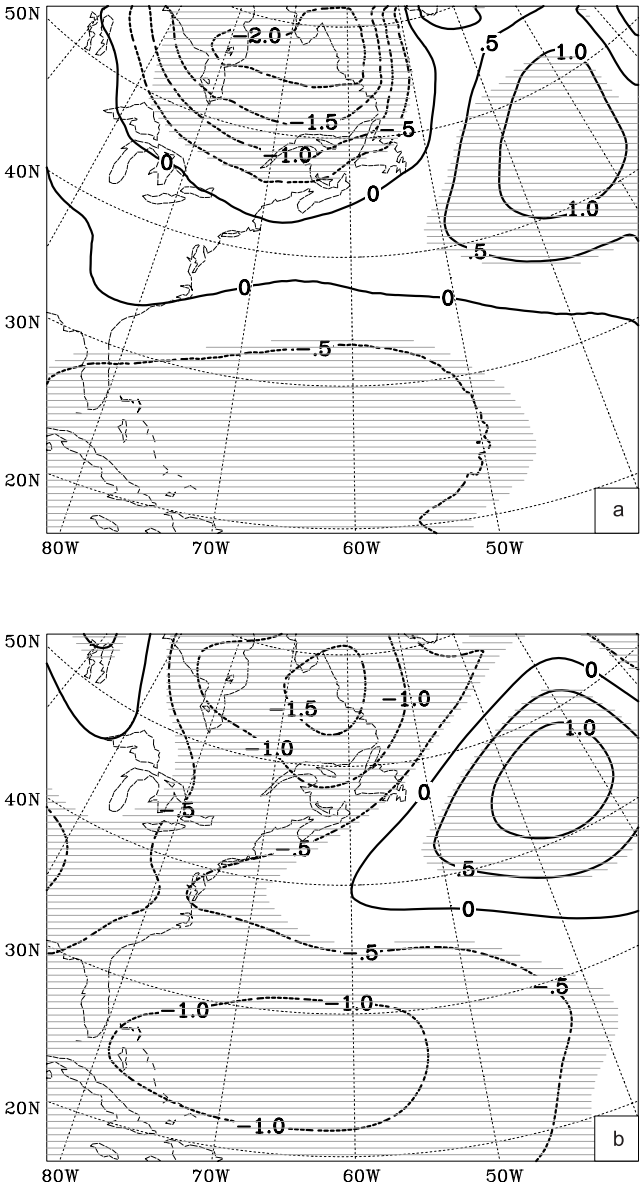

Figure 7. Difference of winter (DJF) SLP, future climate minus current climate: (a) CRCM and (b) CGCM2. Light hatching indicates 95% significance level with Student's t-test. Interval: 0.5 hPa.

which extends in the meridional direction. An associated subtropical SLP decrease also occurs, which can be related to upper tropospheric warming [*Boer et al.*, 1992]. Moreover, significant warming over the northern boundary is also related to the boundary conditions driving the CRCM; thus reductions in temperature gradient between the northern boundary and the ocean in CRCM are largely driven by the CGCM2 boundary conditions.

5.2. Baroclinicity

[26] Comparisons between CRCM and CGCM2 simulations suggest that the two models show similar patterns of change in baroclinicity (Figures 9a–9b). In this discussion, we are concerned with changes in overall baroclinicity, without discerning the impacts on cyclonic and anticyclonic events. In the lower troposphere, there is a significant decrease in the baroclinicity along the east coast of North America, consistent with the change in the temperature gradient shown in Figure 8. To further confirm the impact of temperature gradient, Figure 9c shows the change in Eady Growth rate associated with horizontal temperature gradients simulated by CRCM. Comparisons between Figures 9a and 9c suggest about 80% of the change in the Eady growth rate is related changes in the temperature gradient. Similar results can also be found for the CGCM2 simulation (figure not shown). This suggests that the low-resolution CGCM2 is capturing a similar response to global warming as obtained by higher resolution AR4 models, but with some difference in magnitude. In the upper troposphere, both models suggest enhanced baroclinicity which can tend to offset the impact of decreased lower tropospheric

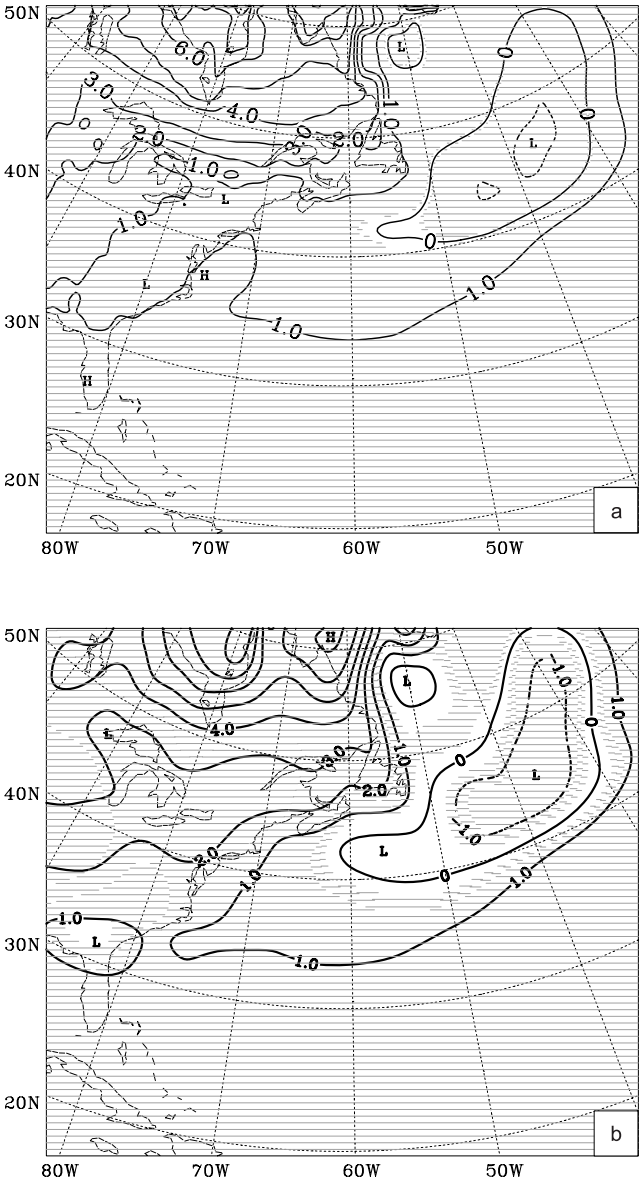

Figure 8. Difference in surface temperature during winter, for future GHG-warmed climate minus present climate, (a) CRCM and (b) CGCM2. Interval: 1°C, the light shading indicates 95% significance level with Student's t-test.

baroclinicity (not shown). However, as mentioned earlier, as baroclinic wave activity is more sensitive to lower level changes than changes in the upper troposphere [*Held and O'Brien*, 1992; *Lunkeit et al.*, 1998], there will be a decrease in midlatitude cyclone activity along the east coast.

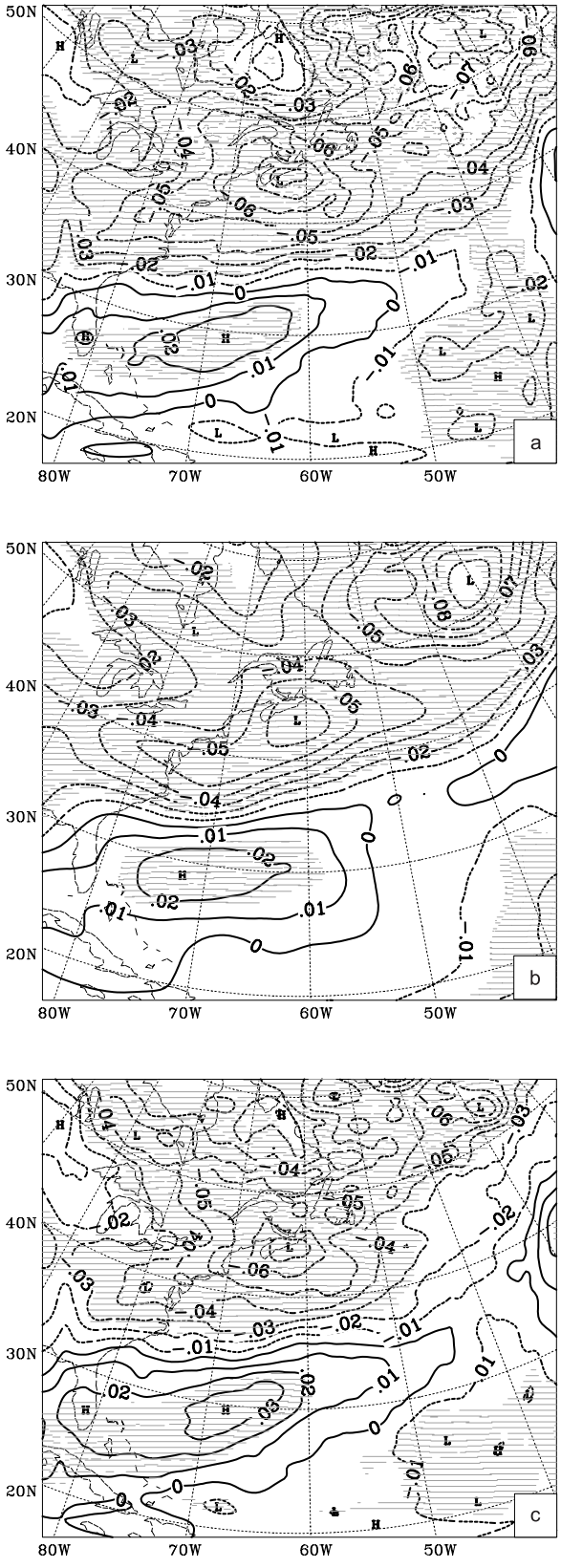

Figure 9. Difference of winter Eady growth rate, estimated from the data at 700 and 850 hPa (future climate minus present climate). Isoline spacing is 0.01 day^{-1}. Light hatching indicates 95% significance level with Student's t-test: (a) CRCM and (b) CGCM2. (c). As in Figure 9a. Difference of winter Eady growth rate from data at 700 and 850 hPa (future climate minus present climate) for CRCM, but only with contributions from horizontal temperature gradient. Isoline spacing is 0.01 day^{-1}.

[27] Besides the changes in the lower tropospheric baroclinicity, changes in moisture content can also potentially influence the storm climate. Although CRCM simulations have more varied results than those of CGCM2, the climate change patterns for specific humidity simulated by the two models are similar. The specific humidity increases everywhere for both simulations. The increase is about 20% in the subtropics and 10% along the east coast of North America (figures not shown). However, it still needs to be proven that this change can lead to an increase in the frequency of intense extratropical storms, or an increase in storm intensity in terms of winds or depth of pressure, in climate change scenarios.

5.3. Track Density

[28] Changes in total cyclone track densities in the climate change scenario, as simulated by the two models, are shown in Figures 10a–10b. CRCM simulations suggest that the number of cyclone tracks is reduced in a warmer climate (Figure 10a) and the largest decrease occurs along the Northwest Atlantic storm track, particularly along the Canadian east coast. Northwest of this reduction area, there are a few small regions where the cyclone track density appears to increase, suggesting slight shifts in storm tracks. However, these regions are not statistically significant. Figure 10b shows that the overall reduction pattern in CGCM2 results is quite similar to that shown in CRCM results. However, the magnitude of the decrease in CGCM2 results is very weak compared to that shown by CRCM. In CGCM2 results, most of areas with statistically significant reduction in track density are located to the east of Newfoundland between 30–50°W. The reduction is about 10% weaker than CRCM results.

[29] The pattern of change in cyclone track density suggested by CRCM results is consistent with GCM simulations reported by *Carnell and Senior* [1998], *Sinclair and Watterson* [1999] and *Bengtsson et al.* [2006]. In particular, *Bengtsson et al.* [2006] suggest that the poleward shift of the storm track over the North Atlantic produces a reduction of storm frequencies along the Canadian east coast which is consistent with the changes observed during 1958–2001, reported by *Wang et al.* [2006]. The latter suggest that both NCEP-NCAR and ECMWF reanalyses show a significant decreasing trend in the number of winter midlatitude cyclones over the midlatitude Northwest Atlantic during 1958–2001, which can be partially attributed to a poleward shift in storm tracks. Study by *Yin* [2005] suggest there is a zonally averaged poleward shift of the jet stream and also a robust poleward shift of the storm tracks in the A1B climate change scenario. To make further comparisons with the study by *Yin* [2005], Figure 11 shows the wind

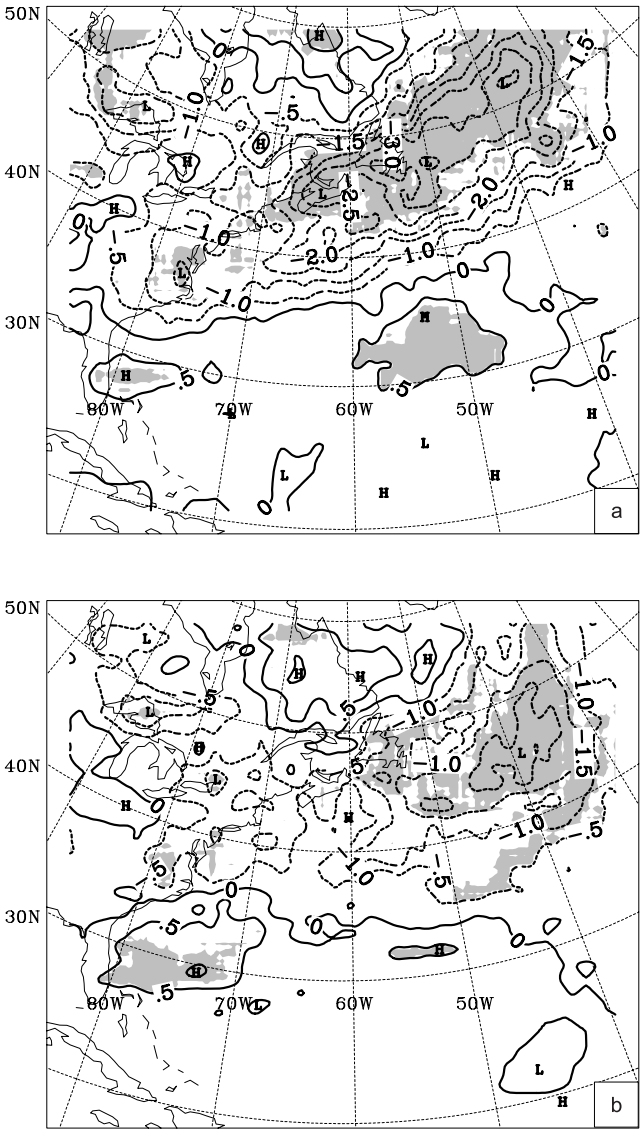

Figure 10. Difference of total cyclone track densities between future climate minus present climate as simulated by (a) CRCM and (b) CGCM2. Interval is 0.5 event per winter. The area with significant level above 95% is shaded.

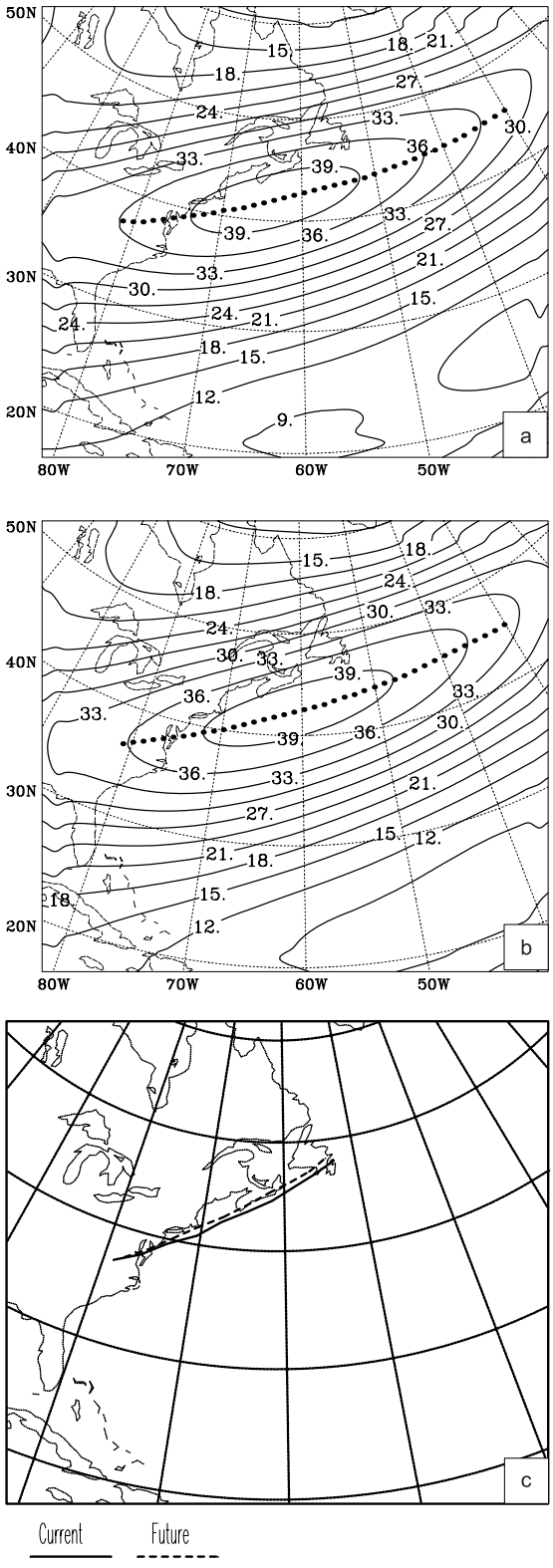

Figure 11. Wind speed at 250 hPa and mean storm track simulated by CRCM for (a) current climate and (b) future climate. Unit: m/s. Bold dotted lines in Figures 11a and 11b are axes of the Jet Stream. (c) Following Figures 11a and 11b, mean storm tracks estimated with the k cluster method.

speed at 250 hPa and the mean storm tracks estimated with the k clustering method in CRCM simulations [*Blender et al.*, 1997]. In Figure 11, we can see a *northeast*ward shift of the jet stream along the east coast of North America while the winter storm track also slightly shifts *northwest*ward. This is consistent with the results from higher resolution AR4 model simulations. Similar results can be found in CGCM simulations (figures not shown). However, the shift of the storm tracks in Figure 11c is not as significant as that shown by *Yin* [2005]. One reason for this result may be related to the fact that the maximum increase in track densities seen in the study by *Bengtsson et al.* [2006] is located outside the CRCM northern boundary.

5.4. Intensities of Midlatitude Cyclones

[30] Under IPCC IS92a scenario conditions, CRCM simulations suggest that cyclone frequencies will decrease in

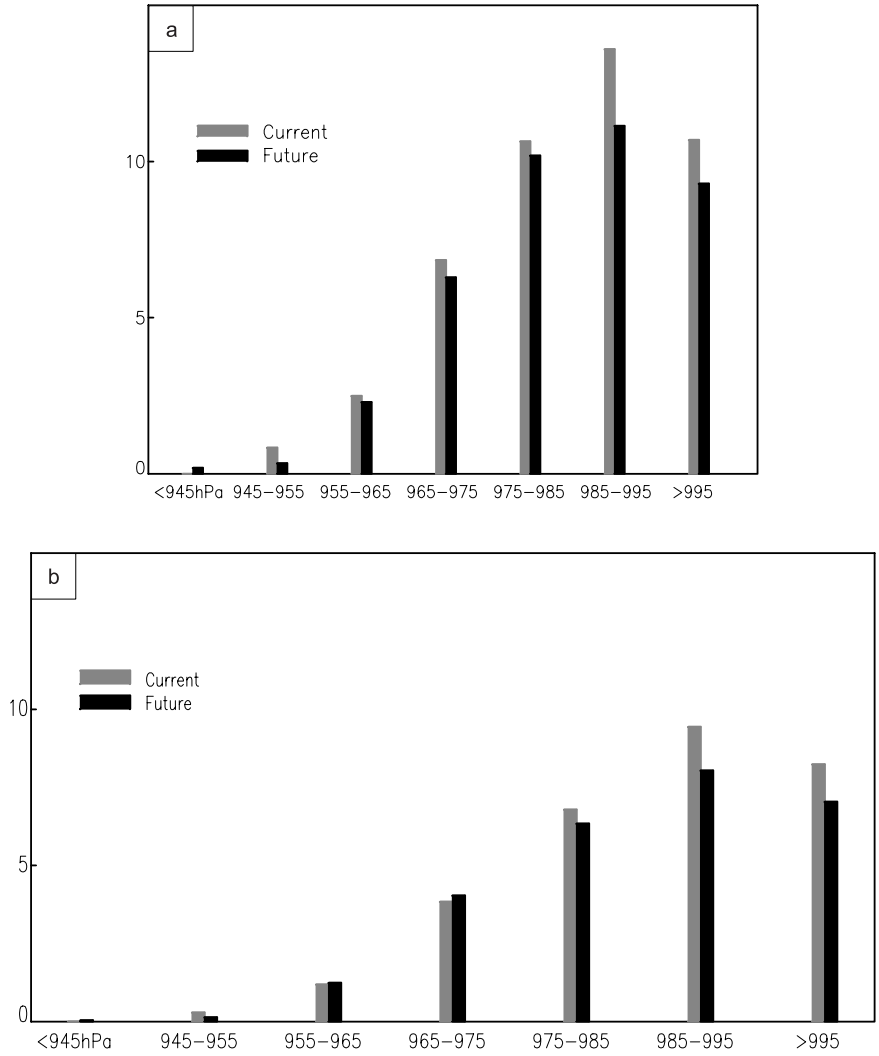

Figure 12. Frequencies of minimum SLP for extratropical cyclones simulated by (a) CRCM and (b) CGCM2, expressed as cyclone occurrences per winter.

almost all pressure bands, particularly the weak cyclones with central pressure higher than 975 hPa (Figures 12a). CRCM results suggest a total of 45 cyclones per winter in the control climate and 40 in the future climate, which is a reduction of 11%. Of these, CRCM simulated 6.7 relatively intense cyclones per winter (with central pressure <970 hPa) in the control climate and 5.4 in the future climate, a 19% reduction. There are four extreme cyclones with central pressure lower than 945 hPa in the GHG-warmed climate, while no such cyclones occur in the control climate. This is consistent with CGCM2 results reported by *Lambert* [2004]. However, the change in the extreme cyclone frequencies is not statistically significant. By comparison, Figure 12b shows that in the GHG-warmed climate, CGCM2 simulates fewer weak cyclones but increased numbers of intense cyclones, compared to the control climate. In total, there are 30 cyclones per winter in the control climate and 27 in the future climate, which is a 10% reduction. For very intense cyclones, the CGCM2 simulation suggests 3 cyclones per winter in the control climate and 3.5 in the GHG-warmed climate, an increase of 17%. Although this result is opposite to the results obtained from the CRCM simulations, the numbers are so small that it is not possible to complete a t test for statistical significance.

[31] Figures 13a–13b compare area distributions of the track density changes of "intense" cyclones (with central SLP less than 970 hPa) from CRCM and CGCM2 simulations, showing track density differences for future climate minus the control climate. While CRCM simulations show a reduction in intense cyclone track density along the dominant storm track in the climate change scenario, there are no clear changes in the CGCM2 estimates.

6. Conclusions

[32] Our main results are that the under climate change scenarios related to global warming the frequency of cyclones may decrease off the east coast of North America in association with reduction in baroclinicity, in agreement with a number of recent studies [*Teng et al.*, 2008; *Geng and Sugi*, 2003]. The novelty of our approach is that a regional climate model is used to downscale results from the coupled GCM which was ran at a relatively coarse resolution. Specifically, we used CRCM and CGCM2 model

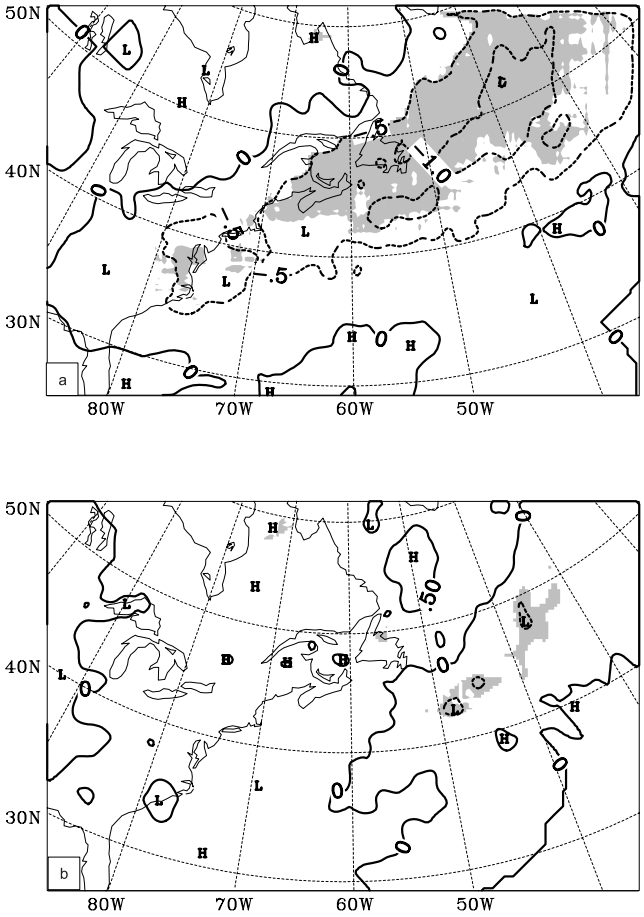

Figure 13. Track density difference of intense extratropical cyclones (with central SLP less than 970 hPa), as simulated by (a) CRCM and (b) CGCM2. Interval is 0.5 cyclone event per winter. The area with significant level above 95% is shaded.

simulations to study the impacts of climate change on midlatitude cyclone activity over the Northwest Atlantic, following the IPCC IS92a scenario. CRCM was implemented on a regional domain, nested within CGCM2. Winter storms were selected from the model outputs for control climate (represented by 1975–1994) and future climate (2040–2059), using automatic storm detection criteria based on SLP. Estimates of the storm climate for the control period were verified with NARR data. Comparisons suggest that both CRCM and CGCM2 are reasonably capable of simulating the control storm climate, reproducing the overall SLP patterns found in NARR data. Both NARR and the model simulations show a distinct maximum baroclinicity along the east coast. However, the CRCM simulation of storm track density achieves better agreement with the NARR data than is achieved by the CGCM2 results. Although both models underestimate the intense cyclone density along the east coast, the bias in CGCM2 results is larger.

[33] Comparisons between CRCM and CGCM2 simulations of the control and future climates suggest that the models share similar patterns of change in variables such as SLP, sea surface temperature, baroclinicity and specific humidity. Although both CRCM and CGCM2 suggest a decrease in cyclone track density, results are more robust in the CRCM results than those of CGCM2. Under the climate change scenario, CRCM simulations suggest that cyclone frequencies will decrease in almost all pressure bands, particularly the weak cyclones. The total estimated reduction is by up to 11% for our area of study, whereas most GCMs predict a reduction of 2–3% globally.

[34] Therefore we suggest that high-resolution CRCM simulations are a useful alternative in estimating the midlatitude cyclone climate along the east coast of North America, compared to coarse resolution GCM studies. Although the overall CRCM results are similar to those of the coarse resolution CGCM2 results, CRCM provides a significant improvement in estimating the climate of intense midlatitude cyclones. Higher resolution in CRCM results is an important factor. For the GHG-warmed climate, changes in the storm climate along the east coast are more statistically significant in CRCM results. The latter are also consistent with previous studies regarding the impacts of climate change on lower tropospheric baroclinicity and midlatitude cyclones in a GHG-warmed climate.

[35] Compared to previous studies [*Yin*, 2005; *Bengtsson et al.*, 2006], we report some differences in terms of changes in baroclinicity and track densities. Previous studies show a northwest shift of storm tracks along the east coast of North America [*Teng et al.*, 2008]. Although we see a similar shift in this study, it is not statistically significant. Part of the reason could be related to the fact that the maximum increase in track densities is located outside of our domain. Furthermore, *Teng et al.* [2008] also suggest an increase in track densities over eastern Canada extending from the Great Lakes eastward to the East Coast, but this increase is absent here. Therefore there are still some uncertainties with the model results.

[36] Studies by *Teng et al.* [2008] suggest that there are differences between A1B climate scenario ensemble members; their results from one-member studies show slight increases in baroclinicity over eastern Canada while their ensemble mean results show a slight decrease. Therefore, in order to test the robustness of our findings, analysis over an ensemble of RCM simulations is required. However, these ensemble simulations at the resolution used in this study (30 km) are not yet available. The number of North American simulations will soon be increased by the new North American Regional Climate Change Assessment Program (NARCCAP; www.narccap.ucar.edu). This program will generate multimodel RCM simulations for both control and future climate. High-resolution model studies by *Bengtsson et al.* [2007] suggest that 30-year integrations may be needed in order to produce robust signals, particularly in regions with relatively low storm densities.

[37] **Acknowledgments.** This work was funded by the Canadian Panel on Energy Research and Development (PERD) for "Extreme Storms and Waves", the Canadian Climate Action Fund (CCAF), and by a CFCAS (Canadian Foundation on Climate and Atmospheric Studies) grant to McGill University on "Diagnostic analyses of water vapour, and its dynamical impact on extratropical transitions".

References

Anderson, D., K. I. Hodges, and B. J. Hoskins (2003), Sensitivity of feature-based analysis methods of storm tracks to the form of background field removal, *Mon. Weather Rev.*, *131*, 565–573.

Bauer, M., and A. D. D. Genio (2006), Composite analysis of winter cyclones in a GCM: Influence on climatological humidity, *J. Clim.*, *19*, 1652–1672.

Beersma, J. J., K. M. Rider, G. J. Komen, K. Kaas, and V. V. Kharin (1997), An analysis of extratropical storms in the North Atlantic region as simulated in a control and 2 × CO_2 time-slice experiment with a high-resolution atmospheric model, *Tellus*, *49A*, 347–361.

Bengtsson, L., K. I. Hodges, and E. Roeckner (2006), Storm tracks and climate change, *J. Clim.*, *19*, 3518–3543.

Bengtsson, L., K. Hodges, M. Esch, N. Keenlyside, L. Kornblueh, J.-J. Luo, and T. Yamagata (2007), How may tropical cyclones change in a warmer climate?, *Tellus*, *59A*, 539–561.

Bengtsson, L., K. I. Hodges, and N. Keenlyside (2009), Will extra-tropical storms intensify in a warmer climate, *J. Clim.*, *22*, 2276–2301.

Blender, R., and M. Schubert (2000), Cyclone tracking in different spatial and temporal resolutions, *Mon. Weather Rev.*, *128*, 377–384.

Blender, R., et al. (1997), Identification of cyclone-track regimes in the North Atlantic, *Q. J. R. Meteorol. Soc.*, *123*, 727–741.

Boer, G. J., N. A. McFarlane, and M. Lazare (1992), Greenhouse gas-induced climate change simulated with CCC second-generation general circulation model, *J. Clim.*, *5*, 1045–1077.

Carnell, R. E., and C. A. Senior (1998), Changes in mid-latitude variability due to increasing greenhourse gases and sulphate aerosols, *Clim. Dyn.*, *14*, 369–383.

Caya, D., and S. Biner (2004), Internal variability of RCM simulations over an annual cycle, *Clim. Dyn.*, *22*, 33–46.

Caya, D., and R. Laprise (1999), A semi-Lagrangian semi-implicit regional climate model: The Canadian RCM, *Mon. Weather Rev.*, *127*, 341–362.

Denis, B., R. Laprise, D. Caya, and J. Cote (2002), Downscaling ability of one-way nested regional climate models: The big-brother experiment, *Clim. Dyn.*, *18*, 627–646.

Flato, G. M., and W. D. Hibler III (1992), Modeling pack ice as a cavitating fluid, *J. Phys. Oceanogr.*, *22*, 626–651.

Flato, G. M., and G. J. Boer (2001), Warming asymmetry in climate change simulations, *Geophys. Res. Lett.*, *28*, 195–198.

Flato, G. M., G. J. Boer, W. G. Lee, N. A. McFarlance, D. Ramsden, M. C. Reader, and A. J. Weaver (2000), The Canadian Centre for Climate Modelling and Analysis global coupled model and its climate, *Clim. Dyn.*, *16*, 451–467.

Gal-Chen, T., and R. C. Sommerville (1975), on the use of a coordinate transformation for the solution of Navier-Stokes, *J. Comput. Phys.*, *17*, 209–228.

Geng, Q. Z., and M. Sugi (2003), Possible change of extratropical cyclone activity due to enhanced greenhouse gases and sulfate aerosols—study with a high-resolution AGCM, *J. Clim.*, *16*, 2262–2274.

Gulev, S. k., O. Zolina, and S. Grigoriev (2001), Extratropical cyclone variability in the Northern Hemisphere winter from the NCEP/NCAR reanalysis data, *Clim. Dyn.*, *17*, 795–809.

Held, I. M., and E. O. O'Brien (1992), Quasigeostrophic turbulence in a three-layer-model: Effects of vertical structure in the mean shear, *J. Atmos. Sci.*, *49*, 1861–1870.

Hodges, K. I., B. J. Hoskins, J. Boyle, and C. Thorncroft (2003), A comparison of recent reanalysis datasets using objective feature tracking: Storm tracks and tropical easterly waves, *Mon. Weather Rev.*, *131*, 2012–2037.

Hoskins, B. J., and K. I. Hodges (2002), New perspectives on the Northern Hemisphere winter storm tracks, *J. Atmos. Sci.*, *59*, 1041–1061.

Hoskins, B. J., and P. J. Valdes (1990), On the existence of storm tracks, *J. Atmos. Sci.*, *47*, 228–241.

Kain, J. S., and J. M. Fritsch (1990), A one-dimensional entraining/detraining plume model and application in convective parametrization, *J. Atmos. Sci.*, *47*, 2784–2802.

Knippertz, P., U. Ulbrich, and P. Speth (2000), Changing cyclones and surface wind speeds over the north-Atlantic and Europe in a transient GHG experiment, *Clim. Res.*, *15*, 109–122.

Lambert, S. J. (1995), The effect of enhanced greenhouse warming on winter cyclone frequencies and strengths, *J. Clim.*, *8*, 1447–1452.

Lambert, S. J. (2004), Changes in winter cyclone frequencies and strengths in transient enhanced greenhouse warming simulations using two coupled climate models, *Atmos. Ocean*, *42*, 173–181.

Laprise, R., D. Caya, A. Frigon, and D. Paquin (2003), Current and perturbed climate as simulated by the second-generation Canadian Regional Climate Model (CRCM-II) over northwestern North America, *Clim. Dyn.*, *21*, 405–421.

Lindzen, R. S., and B. Farrell (1980), A simple approximate result for the maximum growth rate of baroclinic instabilities, *J. Atmos. Sci.*, *37*, 1648–1654.

Lionello, P., and F. Giorgi (2007), Winter precipitation and cyclones in the Mediterranean region: Future climate scenarios in a regional model, *Adv. Geosci.*, *12*, 153–158.

Lunkeit, F., K. Fraedrich, and S. E. Bauer (1998), Storm tracks in a warmer climate: Sensitivity studies with a simplified global circulation model, *Clim. Dyn.*, *14*, 813–826.

McFarlane, N. A., G. J. Boer, J. P. Blanchet, and M. Lazare (1992), The Canadian Climate Centre Second Generation General Circulation Model and its equilibrium climate, *J. Clim.*, *5*, 1013–1044.

Meehl, G. A., et al. (2007), Global climate projections, in *Climate Change 2007: The Physical Science Basis: Contribution of Working Group I to the Fourth Assessment Report of the Intergovernmental Panel on Climate Change*, edited by S. Solomon et al., pp. 747–845, Cambridge Univ. Press, Cambridge, U. K.

Mesinger, F., et al. (2006), North American Regional Reanalysis, *Bull. Am. Meteorol. Soc.*, *87*, 343–360.

Mitchell, J. F. B., T. C. Johns, J. M. Gregory, and S. F. B. Tett (1995), Climate response to increasing levels of greenhouse gases and sulphate aerosols, *Nature*, *376*, 501–504.

Muskulus, M., and D. Jacob (2005), Tracking cyclones in regional model data: The future of Mediterranean storms, *Adv. Geosci.*, *2*, 13–19.

Pacanowski, R. C., K. Dixon, and A. Rosati (1993), The GFDL Modular Ocean Model Users Guide, *GFDL Ocean Group Tech. Rep. 2*, 46 pp., Geophys. Fluid Dynamics Lab., Princeton, N. J.

Pan, Z., J. H. Christensen, R. W. Arritt, W. J. Gutowski Jr., E. S. Takle, and F. Otieno (2001), Evaluation of uncertainties in regional climate change simulations, *J. Geophys. Res.*, *106*, 17,735–17,751.

Paquin, D., and D. Caya (2000), New convection scheme in the Canadian Regional Climate Model. Research activities in atmospheric and oceanic modelling, WMO/TD-987, *Rep. 30*, pp. 7.14–7.15, World Meteorol. Organ.

Plummer, D. A., D. Caya, A. Frigon, H. Côté, M. Giguère, D. Paquin, S. Biner, R. Harvey, and R. de Elía (2006), Climate and climate change over North America as simulated by the Canadian Regional Climate Model, *J. Clim.*, *19*, 3112–3132.

Schubert, M., J. Perlwitz, R. Blender, K. Fraedrich, and F. Lunkeit (1998), North Atlantic cyclones in CO_2 induced warm climate simulations: Frequency, intensity, and tracks, *Clim. Dyn.*, *14*, 827–837.

Semmler, T., et al. (2008), Regional climate model simulations of Noth Atlantic cyclones: Frequency and intensity changes, *Clim. Res.*, *36*, 1–16.

Shaffrey, L., et al. (2009), UK-HiGEM: The new UK high resolution global environment model: Model description and basic evaluation, *J. Clim.*, *22*, 1861–1896.

Sinclair, M. R. (1994), An objective cyclone climatology for the Southern Hemisphere, *Mon. Weather Rev.*, *122*, 2239–2256.

Sinclair, M. R., and I. G. Watterson (1999), Objective assessment of extratropical weather systems in simulated climates, *J. Clim.*, *12*, 3467–3485.

Stouffer, R. J. (2004), Time scales of climate response, *J. Clim.*, *17*, 209–217.

Teng, H., W. M. Washington, and G. A. Meehl (2008), Interannual variations and future change of wintertime extratropical cyclone activity over North America in CCSM3, *Clim. Dyn.*, *30*, 673–686.

Ulbrich, U., and M. Christoph (1999), A shift of the NAO and increasing storm track activity over Europe due to anthropogenic greenhouse gas forcing, *Clim. Dyn.*, *15*, 551–559.

Wang, X., V. R. Swail, and F. W. Zwiers (2006), Climatology and changes of extratropical cyclones activity: Comparison of ERA-40 with NCEP-NCAR reanalysis for 1958–2001, *J. Clim.*, *19*, 3145–3166.

Wernli, H., and C. Schwierz (2006), Surface cyclones in the ERA40 data set (1958–2001). Part I: Novel identification method and global climatology, *J. Atmos. Sci.*, *63*, 2486–2507.

Yin, J. (2005), A consistent poleward shift of the storm tracks in simulations of 21st century climate, *Geophys. Res. Lett.*, *32*, L18701, doi:10.1029/2005GL023684.

Zhang, Y., and W. Wang (1997), Model-simulated northern winter cyclone and anticyclone activity under a greenhouse warming scenario, *J. Clim.*, *10*, 1616–1634.

Zisha, K. M., and P. J. Smith (1980), The climatology of cyclones and anticyclones over North America and surrounding ocean environs for January and July, 1950–1970, *Mon. Weather Rev.*, *108*, 387–401.

Zolina, O., and S. K. Gulev (2002), Improving the accuracy of mapping cyclone numbers and frequencies, *Mon. Weather Rev.*, *130*, 748–759.

D. Caya, Centre pour l'Étude et la Simulation du Climat à l'Échelle Régionale (ESCER), Université du Québec à Montréal, P.O. Box 8888, Station Downtown, Montréal, QC, Canada H3C 3P8.

J. Gyakum, Department of Atmospheric and Oceanic Sciences, McGill University, 805 Sherbrooke Street West, Montreal, QC, Canada H3A 2K6.

R. Laprise, Département des Sciences de la Terre et de l'Atmosphère, Université du Québec à Montréal, P.O. Box 8888, Station Downtown, Montréal, QC, Canada H3C 3P8.

Z. Long and W. Perrie, Fisheries and Oceans Canada, Bedford Institute of Oceanography, 1 Challenger Drive, P.O. Box 1035, Dartmouth, NS B2Y 4A2, Canada. (perriew@dfo-mpo.gc.ca)